PYRAMID COARSE SUN SENSING FOR NASA SSTI "CLARK" SAFE-HOLD MODE

Jeff Benton
CTA Space Systems
McLean, Virginia

Abstract

This paper describes an innovative approach to solving the Sun-pointing problem using a pyramid configuration of Coarse Sun Sensor (CSS) cells. In safe-hold mode, the Small Spacecraft Technology Initiative (SSTI) Clark spacecraft must keep its solar arrays towards the Sun using only CSS cells to sense the Sun. Unfortunately, Earth albedo degrades the accuracy of the Sun vector from these cells. Two CSS configurations are considered. A traditional configuration has cells mounted flat on each spacecraft face, with their normals along the spacecraft body axes. An alternative configuration has cells on the face of a shielded pyramid as well as the flat-mounted cells. A simulation is used to evaluate the safe-hold pointing performance with these two configurations. The CSS models generate illumination values while the CSS algorithms use these values to build a sensed Sun vector. The sensor models approximate illumination from the Earth albedo as well as from the Sun. The flat-mounted configuration is compared with the pyramid (plus flat-mounted) configuration of CSS cells. Although the flat-mounted configuration satisfies the Clark requirements, the pyramid configuration reduces Sun pointing safe-hold performance errors by 50%. Moreover, the pyramid CSS configuration is robust to errors from the widely varying Earth albedo.

I. Overview of Clark Safe-hold Mode

The Clark spacecraft has two safe-hold modes: safe-hold 0 and safe-hold 1. Each mode can employ either coarse or fine attitude control. The coarse Sun sensing is traditionally associated with the coarse control in safe-hold 0. For the rest of this paper, the words "safe-hold" will refer to this coarse control.

In safe-hold, the task of Clark's ACS (Attitude Control System) is to point its solar arrays towards the Sun so as to maintain charge on its batteries. To do this, Clark's panels remain in the index position (panel normals approximately along the spacecraft's -Z axis). The spacecraft attitude is then Sun pointing instead of Earth pointing, as in normal mode. To minimize structure flexibility problems, Clark is powered by relatively small solar panels augmented by reflectors to focus the Sun's light onto the panels. As the panel normals diverge from the Sun, power from the reflector equipped panels drops more quickly than it would for unfocussed panels. Although the initial goal was to keep the Sun pointing error within 10°, less stringent power requirements have enabled us to relax this goal to about 20°.

Clark's safe-hold philosophy of using simple sensors with hearty flight heritage limits it to using the TAM (Three Axis Magnetometer) and CSSs (Coarse Sun Sensors) for this Sun pointing.

The TAM senses spacecraft attitude rates about the Sun line, while the CSSs sense both rate and attitude position. Without access to the Sun, Clark's safe-hold ACS ignores attitude errors in eclipse. In eclipse it merely attempts to keep its rates down and reduce its wheel momenta. Since Clark's attitude is uncontrolled in eclipse, it needs its CSS cells to re-acquire the Sun after each orbit sunrise.

A Treetops™ (Dynacs Engineering Co., Inc., Clearwater, Florida) dynamic control simulation was used to evaluate the safe-hold pointing performance. This simulation of the Clark ACS contains both the CSS model and the CSS algorithms. The CSS models generate illumination values from the CSS cells while the CSS algorithms use these values to build a sensed Sun vector. To realistically generate illumination values, the CSS models must account for deficiencies in the cells' measurements of the Sun's light.

II. Deficiencies of Coarse Sun Sensor Cells

In building a Sun vector with only Clark's coarse Sun sensors, the ACS engineer must overcome three sensor deficiencies. First, Sun light reflected from the Earth, i.e., the Earth albedo, corrupts the Sun vector. Second, the signal from the CSS cells drops to zero for illumination within 7° of the cell face. Third, the CSS cells lose their sensitivity to the direction of the Sun vector when it is close the cell normal. Discussions of each these deficiencies follow below. The Earth albedo is the most complicated, uncertain, and difficult to model of the three.

Corruption by Earth Albedo

There seem to be two uses of the word albedo. One is the Earth's light received by the spacecraft. The other is the light from any one patch of the Earth's atmosphere. Both are a ratio of the Earth light to Sun light. In this paper "albedo" will generally refer to the light from a patch of the Earth while "albedo vector" will refer to the Earth's light received by spacecraft.

Since the spectrum of the Earth albedo is very close to the spectrum of the Sun's light, the CSS cells respond to albedo almost as readily as they do to the Sun. [1] Furthermore, since the cells have an approximately 2 pi steradian field of view, a cell can frequently see the Sun and Earth simultaneously. The Sun and albedo vectors then combine to yield an incorrect Sun vector as seen by a CSS cell.

The controller's CSS algorithm was specifically designed to reject the Earth's albedo in calculating the Sun vector. Thus, to test this algorithm, considerable attention was devoted to properly simulating this albedo. Given the Sun and Earth vectors, the albedo model generates the CSS output signals due to Earth illumination. Then, the CSS subroutine combines these signals with those due to the Sun illumination to build complete illumination measurements for each CSS cell.

Albedo Models

The preliminary model of the Earth albedo consisted of a vector, from the center of the Earth to the spacecraft, whose magnitude remained constant throughout the Sun lit portion of the orbit. This model was too crude yielding considerably worse than worst case results. The current model incorporates four adjustments to this original model. Three adjustments account for: the variable area of the visible lit Earth, the Sun angle of incidence on the Earth, and the direction of the albedo vector (from the center of illumination of the lit Earth). [2] The fourth adjustment is the table of albedo intensities originally from "Earth Radiation Budgets". [3]

The table as reprinted in the Satellite Thermal Control Handbook, which includes estimated albedos at polar latitudes, is the table used in the simulation. [4]

The first three of the four adjustments unequivocally reduce the magnitude of the Sun pointing error from the first model, the nadir pointing Earth albedo. Paul R. Spencer's paper provided these three albedo adjustments. [2] The albedo work in Spencer's paper assumes that the Sun is in the orbit plane. Clark's orbit does not quite conform to this assumption: with an 11:15 am (descending node) orbit, the Sun is 11.25° out of the orbit plane. The simulation algorithms faithfully follow Spencer's equations and do not account for this 11.25° beta angle.

More importantly, this 11.25° is irrelevant to the albedo simulation. The calculations of CSS illumination at one instant in Clark's orbit have no bearing on these calculations at any other instant in the orbit. Since these calculations have no memory, Clark's orbit is irrelevant to their accuracy. Only its position with respect to the Earth and the Sun matter in calculating the illumination. Put another way--since the Sun, the Earth, and the spacecraft can always be coplanar with each other--these equations will always apply at any instant. They will apply regardless of whether or not the spacecraft will be in this same plane the next time the simulation applies the equations.

The first adjustment causes the intensity of the albedo on the spacecraft to vary with the size of the area of the Sun lit Earth visible to the spacecraft. As a spacecraft moves out of the Earth's shadow, it first sees a crescent shaped portion of Sun lit Earth. As it approaches the Earth-Sun line, this area grows into a gibbous shape and then a full round circle. Spencer quantifies this effect in his equations B6 to B8.

Next, the algorithm accounts for the angle at which the Sun's light strikes the Earth. As Clark moves towards the Earth-Sun line, the Earth reflects the Sun's light at a sharper and sharper angle approaching the Earth's normal vector. Spencer assumes that the Earth albedo follows Lambert's law for flat diffuse surfaces, i.e., that the albedo intensity decreases with the cosine of the angle of incidence. Therefore, assuming this law, the albedo intensity will increase as the spacecraft approaches the Earth-Sun line. Spencer calculates this factor in equation B11.

For the third adjustment from Spencer's paper, the albedo model disassociates the albedo vector from the nadir vector. Spencer represents the albedo by a vector from the center of the lit Earth portion visible to the spacecraft. When Clark first sees the crescent lit Earth, this vector is rather near the Sun vector. As Clark comes up over the poles, this vector moves towards the nadir vector. The albedo is closest to the nadir vector when the spacecraft is closest to the Earth-Sun line. Spencer's equations for this effect are B10, B12, and B13.

The fourth and final albedo adjustment is to vary the albedo intensity with the latitude of the reflection point (i.e., the center of the visible lit Earth). These intensities come from a table of monthly average Earth albedos measured by five spacecraft. [3] James Wertz indicates that the Earth albedo may vary from "0.05 [5%] for some soil- and vegetation-covered surfaces to over 0.80 [80%] for some types of snow and ice or clouds [Lyle, et. al., 1971]." [1] This variation makes choosing a single number for a multiple orbit simulation difficult. An informal poll of ACS engineers familiar with Low Earth Orbiting (LEO) spacecraft suggests that the light reaching the spacecraft is typically from 15% to 50% for the Earth Albedo. While the albedo varies from 5% to 80%, the spacecraft never sees as much as 80% due to the compounding effects of the first three adjustments discussed above.

The four adjustments move the worst albedo driven error to the time when the spacecraft is roughly midway between the Arctic (or Antarctic) circle and its corresponding pole. It is the worst here because of the combined effects of: a relatively icy ground cover (at the Sun reflection point), a high Sun angle of incidence (on the Earth), an albedo vector that is relatively far from the Sun, and the relatively large visible lit Earth.

Confirmation of Albedo Models

The albedo model, with the four adjustments discussed above, was checked after each adjustment was in place. The interpolation of the albedo intensities was confirmed by checking values observed in the FORTRAN debugger. Verification of each of the other adjustments consisted of sanity checks applied to albedo vectors and magnitudes printed out in debugging statements. Each adjustment ultimately produced reasonable values. Furthermore, after each adjustment, the shape of error curve duplicated Spencer's curve with increasing

fidelity. This increasing fidelity lends confidence to the implementation of these adjustments.

In Fig. 1 is a plot of the angle between the CSS sensed and true Sun vector. This angle, or CSS error, is set to zero in the eclipses. The dashed horizontal line is the average CSS error for the Sunlit portions of the plot only. The average, 5.03°, is above and to the left of this line. The simulation for this plot used the flat-mounted configuration of cells and Sun vector logic in Section III below. Unlike Spencer's plots, this error plot displays a high frequency oscillation. This choppiness is due to the flat-mounted CSS algorithm repeatedly choosing the "wrong side" for one of the Sun vector's components. This phenomena is discussed in Section III, below. Also unlike Spencer's plots, this plot has only one predominant peak, in the first half of the Sun lit portion of the orbit (the Sun pass). This is because Clark flies into the Sun over the northern hemisphere's ice cap in June. When Clark is simulated in December, a similar peak appears only in the second half of the Sun pass, in the southern hemisphere. During the equinoxes though, this Sun error plot exhibits two peaks. One peak is over each hemisphere, as in Spencer's plot.

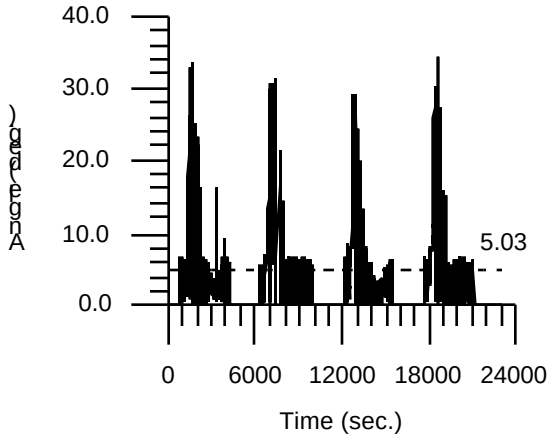

Fig. 1: Angle Between the CSS Sensed and True Sun Vector.

A final assessment of the albedo model can be made by comparing Fig. 1 with a plot of the REX II, on orbit, Sun vector error. REX II is a momentum bias, Earth pointing satellite with CSS cells mounted normal to the spacecraft body axes. It uses the same flat-mounted configuration of cells and Sun vector logic as described in Section III below. The REX II data is the graph in Fig. 2. REX II was built by CTA Space Systems and launched in January of 1996. The data was collected in mid-April of 1996. The narrow gaps in the data occur when REX II is in eclipse while the broad gaps in the data are due to lost or bad data. The data suggests two error peaks, one in each hemisphere, as befits a near polar spacecraft closer to an equinox than to a solstice.

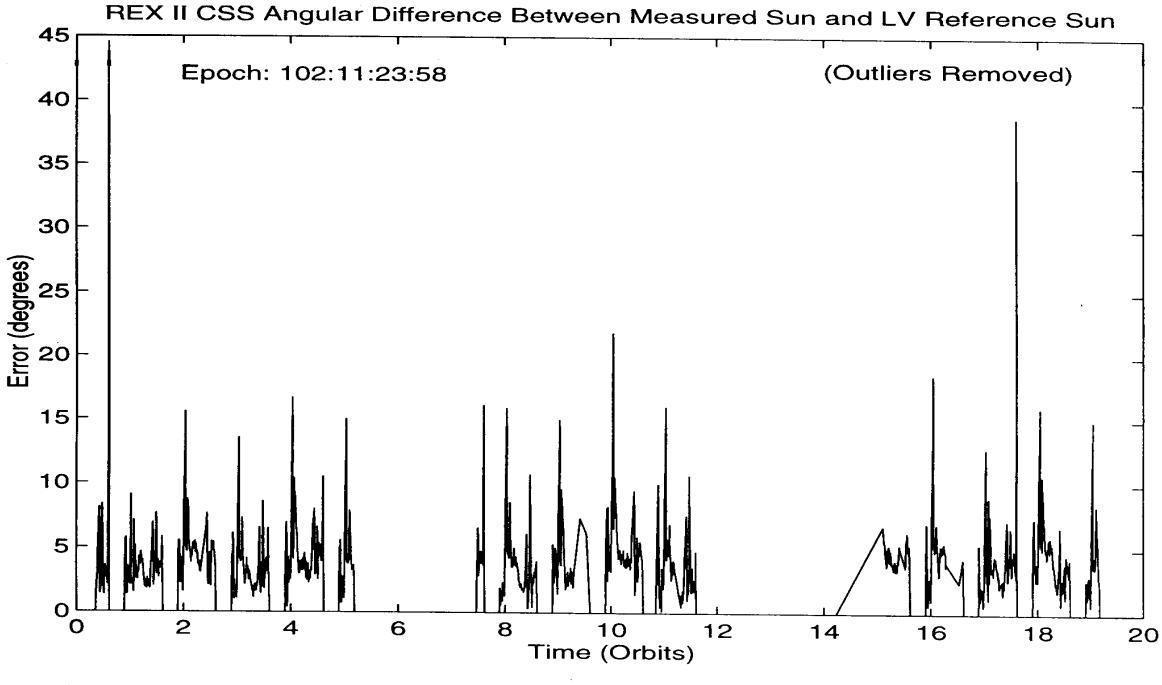

Fig. 2: REX II, On-orbit, Sun Vector Error with Flat-mounted CSS Cells.

Signal Lose for Vectors < 7° Off Cell Face

Next to the Earth albedo, the worst CSS cell deficiency is the "7° dropout". This is a loss of signal if the Sun vector glances the cell within 7° of the cell face. Noise on the sensor harness as well as the thermally driven noise in the signal processing devices causes this dropout. Since electrical noise causes this loss, it will also obscure any low signal from the CSS cells. Thus, near normal illumination of the cell will go undetected if the magnitude of this illumination is less than that of the Sun striking the cell within 7° of its face. The simulation does not account for losses due to reflection from the surface of the CSS cell or other optical losses.

Lose of Sensitivity for Near-normal Vectors

The output from each CSS is approximately the cosine of the angle between the CSS normal vector and the Sun vector. The plot of this output, Fig. 3, clearly indicates the leveling out of the curve as the Sun vector approaches the cell normal.

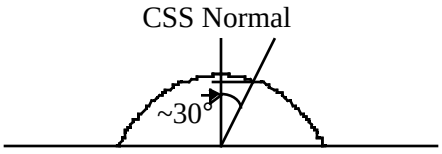

Fig. 3: Angle Between A CSS Normal and An Illumination Vector.

The leveling causes an insensitivity to variations in the CSS reading when the Sun vector is close to the normal.

This insensitivity or uncertainty is exacerbated by the quantization of the CSS output. For example, if a 12 bit Analog to Digital (A/D) Converter converts the CSS

output to digital the least significant bit is 1/4096th, or approximately 0.0002, of full scale. When measuring near the sensor normal (i.e., cosine of 0° 1), the arccosine of (one minus) this uncertainty is approximately 1.27°. However, when measuring only 30° off the normal, this same 0.0002 uncertainty translates into a 0.03° uncertainty. (Uncertainty = Arccosine[cos(30°) - (1/4096)] - 30°)

The three deficiencies, corruption by Earth albedo, loss of signal within 7° of cell tangent, and loss of precision for near normal vectors are applied to each CSS cell in the sensor model. While the calculations for these deficiencies are common to all cells in both configurations, the two different configurations require different models and algorithms.

III. The Flat-Mounted Configuration of Clark's Coarse Sun Sensors

The flat-mounted configuration of CSS cells is a traditional configuration that CTA Space Systems has included on the Meteor, REX I, and REX II spacecraft. This configuration has cells mounted flat on each spacecraft face, with their normals along the spacecraft body axes. The corresponding algorithm chooses orthogonal cells to build its Sun vector.

Sensor Model

The sensor model takes a dot product of the body Sun vector with each of the CSS normal vectors for the Sun's contribution to the illumination of the sensors. After accounting for the Sun's direct light, the model calculates a vector describing the Sun's light reflected from the Earth.

In calculating the albedo vector the model accounts for the: amount of the currently visible lit Earth, the effect of the incidence of Sun light on the Earth, and the albedo's direction. Then it uses the current day and month to interpolate the Earth albedo intensity from the Satellite Thermal Control Handbook. [4]

Having calculated the albedo vector, the model dots this vector with each CSS cell normal vector. The simulation adds these dot products, the Earth's contribution to the illumination of the sensors, to the products from the direct Sun light.

With the sensors now illuminated by both Earth and Sun, the CSS model checks the magnitude of each CSS cell reading. If any reading is less than the sine of 7°, the simulation sets this component to zero. This represents the 7° "drop-out" discussed in Section II, above.

Next, the model adds noise to each output and quantizes it to approximate Clark's Analog to Digital (A/D) conversion. Finally, it returns these values as an array of fourteen CSS outputs.

Sensor Processing Algorithm

While the CSS model generates the CSS illumination values, the CSS algorithm uses these values to build a sensed Sun vector. For the purposes of the flat-mounted CSS algorithm, the Clark spacecraft (excluding her solar arrays) is an oblong, six-sided, rectangular solid.

Each face of the solid has two (or more) CSS cells with their normals along the face normals. At regular intervals, Clark's ACS records CSS values. The CSS algorithm then rejects the darker cells from each face under the assumption that they are shaded by a solar array or some other appendage. (Note that shading effects, such as those of the solar arrays, are not simulated here.)

Having chosen one cell from each face, the algorithm then compares cells from opposing faces. For example, it will compare cells on the positive and negative Z faces as in Fig. 4. Again it rejects the darker cell. Assuming that the less brightly

illuminated face is seeing the Earth albedo while the more brightly illuminated face is seeing the Sun. With the CSS values reduced to those of three orthogonal cells, the algorithm takes each cell's value as a component of the Sun vector in the body frame. Finally, the algorithm unitizes this Sun vector before its use in any attitude control activity.

Fig. 1, the "Angle Between CSS and True Sun [vectors]", demonstrates the two classes of Earth Albedo errors particular to the flat-mounted configuration. The first class of error is a smoothly increasing error as the spacecraft approaches high (but not maximum) latitudes. At high latitudes, vectors from the Sun and the Sun-lit portion of the Earth are close enough together to be well within the CSS field of view. When the CSS sees both the Sun and Earth albedo vectors simultaneously, its reading is a geometric sum of these vectors yielding an erroneous magnitude. The second class of error occurs when the CSS algorithm chooses the "wrong side".

This second class of error results if the spacecraft is oriented such that the Sun hits a face very obliquely while the Earth albedo hits the opposite face very directly. See Fig. 4. In this orientation, the Earth-ward face may register a stronger illumination than the Sun-ward face despite the Sun's greater intensity. The CSS algorithm, mistaking the brighter side for the Sun-lit side, thus chooses the "wrong side" and substantially degrades the body Sun vector. The algorithm usually chooses the "wrong side" for only one of the three axes. An abrupt jump in the Sun vector error marks the moment at which the direct albedo surpasses the oblique Sun light. This error repeats back and forth rapidly due to the fluctuating effect of the random noise simulated in the CSS model.

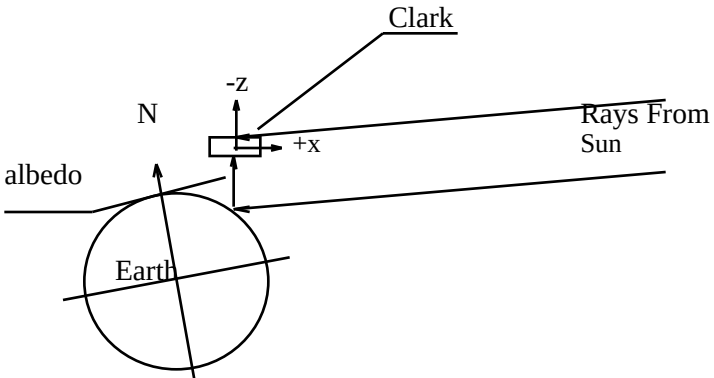

Fig. 4: Albedo Impinging On the Z Face of the Clark Spacecraft.

Fig. 5 shows the results of a simulation using the flat-mounted CSS cells and algorithm. This graph, the True & CSS Panel-Sun Angle graph, plots two values against time. The solid line in this graph is the angle between the panel normal and the (true) Sun vector. This angle jumps to 90° because the CSS sensed Sun vector defaults to $[1, 0, 0]^T$ while the spacecraft is in eclipse. Note also that the true Sun vector is even plotted when the spacecraft is in eclipse. The horizontal dotted (not dashed) line is the average angle between the true Sun vector and the panel normal--averaged over the Sunlit portions of the orbit only. This value, 16.3°, is printed above the line.

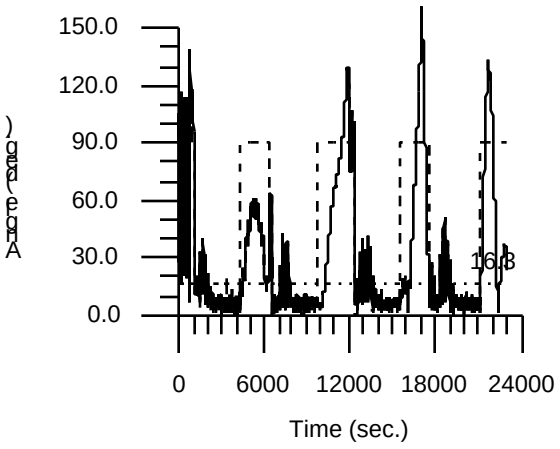

Fig. 5: True & CSS Panel-Sun Angle; Flat-Mounted Configuration.

The graph in Fig. 5 is from a simulation with the nominal values of Earth albedo taken from the table of flight measured values.[4] The simulated orbit is the Clark orbit with a 256.5051 nmi altitude and a 97.297° inclination. The initial conditions are a 0° sweep angle, a 243.6° right ascension of the ascending node, and a date of June 6, 1996. The simulation also begins with the maximum tip-off rates for the deployed spacecraft. (These orbital parameters and initial conditions are the same for all subsequent plots of Clark's safe-hold Sun pointing performance.)

IV. The Pyramid Configuration of Coarse Sun Sensors

The pyramid configuration of CSS cells works in conjunction with flat-mounted CSS cells. While the collar around the pyramid reduces and eliminates the albedo seen by the pyramid sensors, it also limits their field of view of the Sun. See Fig. 6. This configuration uses the flat-mounted cells to bring the Sun into the pyramid's collared field of view.

The Treetops™ simulation of this sensor configuration consisted of modeling the pyramid and simulating the sensor algorithm. The pyramid model calculates the intensities sensed by the pyramid CSS cells while the algorithm determines whether to use the flat-mounted or pyramid arrangement of cells. The algorithm then builds the chosen set of intensities (flat-mounted or pyramid) into a Sun vector.

Sensor Model

The worst errors for the flat-mounted CSS cells were due to the Earth albedo's degradation of the true Sun vector and the loss of signal (dropout) when the illumination vector was within 7° of the sensor face. The tilt of the pyramid faces helps eliminate the 7° dropout while the collar around the pyramid reduces and eliminates the albedo. See Fig. 6 again.

TOP VIEW

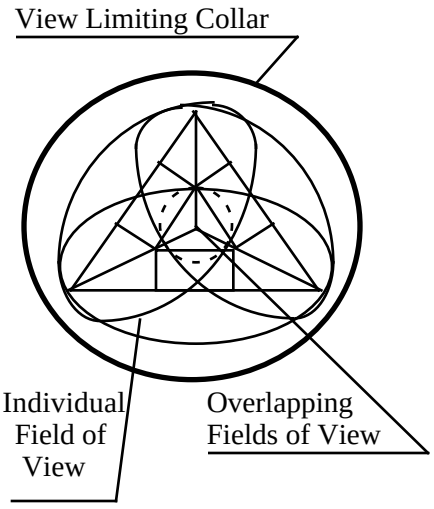

SIDE VIEW

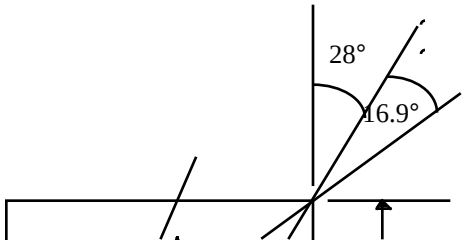

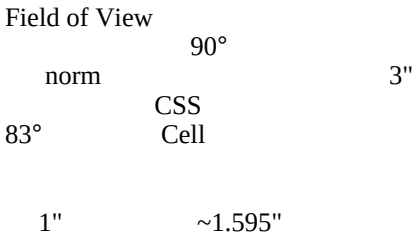

Figure 6: Pyramid of Coarse Sensors with View-Limiting Collar (not to scale).

The primary advantage of the pyramid is that it overlaps each CSS cell's field of view to produce a region free of the 7° dropout. The pyramid has three sides, each of which are perpendicular to the other two. Imagine cube with one of its corners cut off. Then, the detached corner resting flat on its cut face is the shape of the pyramid. The pyramid is on the -Z (zenith) face of the spacecraft. Its base is tilted by - The dashed line is the angle between the panel normal and the CSS measurement of the Sun vector. Note the abrupt jumps in this measured Sun vector, near 4000 seconds for example. 10° about the roll axis so that the pyramid normal (perpendicular to the pyramid base) is parallel to the panel normals. The sensor cells are mounted flat on the sides of the pyramid. Each cell has a 166° (cone diameter) field of view centered about its normal. Since each cell normal is elevated approximately 35.26° from the pyramid base, each cell's field of view overlaps the pyramid normal by approximately 28°. This overlap creates a 56° (diameter) field of view centered on the pyramid normal. This 56° field of view is devoid of 7° dropout regions. Note that any vector that is unlimited by the collar is visible to all three CSS cells of the pyramid.

More important than limiting the CSS cells' 7° dropout zones, the collar also shields them from the Earth albedo. As discussed in section II, the albedo vector comes from the center of the visible lit Earth. As Clark comes up over the poles, this vector moves from the Sun vector towards the nadir vector. Once the albedo is more than 28° from the Sun vector, though, the collar will begin to block it out if the sensor is looking near the Sun, i.e., if the panel-Sun errors are small. The algorithm discussed below looks for suitably small panel-Sun errors before relying on the pyramid configuration. For vectors between 28° and 45° (28° + 16.9°) from the pyramid normal, the collar reduces the illumination. Once the albedo vector is approximately 45° from the Sun vector, the collar will completely block it out for small panel-Sun errors.

When applying either the Sun or albedo to the pyramid, the simulation model first calculates the component of the illumination's unit vector that is normal to the base of the pyramid (and hence normal to the panels).
If this component is less than the cosine of 28° it reduces the magnitude of the vector to simulate the collar's shading. If it is less than the cosine of 45°, the model sets the vector to zero. Then the model dots the illumination vector (Sun or Earth light) with each CSS normal on the pyramid. After applying both Sun and Earth light (as appropriate) to the pyramid, the model applies the 7° drop-out as it did for the flat-mounted cells. Then, the model simulates noise and signal quantization. Finally, before returning control of the simulation to the calling routine, the pyramid model checks to see that each sensor sees at least 15% of the full Sun's intensity. This 15% is approximately the sine of 8.6°, 1.6° more than the 7° dropout. If any one face sees less than 15% the model clears a flag, "PFMIN", to show that the pyramid is not yet suitable for sensing the Sun.

An extra degree of improvement is due to the tilted CSS cells reducing the insensitivity to variations in the measured vector. As discussed in section II, the CSS output is insensitive to variations in a Sun vector near the CSS cell normal. With the view limiting collar and the inclined CSS cells, no full (i.e., collar unlimited) illumination vector can get closer than about 63° from any cell normal. When measuring

63° off the normal, Clark's 12 bit digital measurement uncertainty translates into approximately 0.016° of uncertainty in that one component of the vector. This is approximately 1/80th the uncertainty near the cell normal.

Testing the pyramid sensor model consisted of sanity checks applied to measured and true Sun vectors and magnitudes. These values were observed in the on-line debugger of the FORTRAN language application package. These checks produced reasonable values. Moreover, once the model was complete, the Sun vector error curves closely resembled those from the view-limited (i.e., collared or shaded) sensor in Spencer's article. [2]

Sensor Processing Algorithm

The pyramid CSS algorithm, as opposed to the flat-mounted CSS algorithm, is merely a vector transformation. Since the three pyramid CSS normals are orthogonal to each other, the pyramid CSS readings describe the Sun vector in a Cartesian frame. For convenience, call this the pyramid frame. If each CSS is displaying the minimum reading (15% of full scale), the pyramid CSS algorithm merely transforms the Sun vector into the spacecraft body frame.

The logic that chooses the CSS cell configuration (pyramid or flat-mounted) is in the Appendix. The simulation only executes this logic if Clark is not in eclipse. If in Sun, the logic checks to see if the pyramid sensors are a valid measurement of the Sun vector.

If the pyramid sensors were not valid last control cycle, the logic takes the left branch to check the validity of using the pyramid. It calls the pyramid routine to see if each cell of the pyramid is reading more than the minimum 15% of full scale. Then it checks the flat-mounted CSS cells to see if the Sun appears to be within 25° of the panel normal. If both of these conditions are satisfied (all pyramid cells have at least the minimum reading and the Sun within 25° of the panel normal) the logic sets "PFCSS" ("Pyramid Fix" CSS) to 1 indicating that the pyramid sensors have a valid measurement of the Sun vector. It then calls the pyramid routine again to measure the Sun vector.

If either condition is not satisfied, PFCSS is zero and the algorithm ends with the flat-mounted cells having measured the Sun vector.

If the pyramid sensors were valid during the last control cycle, the logic takes the right branch to get the pyramid sensed Sun vector. It calls the pyramid routine to get this vector. It then checks the PFMIN flag returned by this routine to verify that each face is reading more than the minimum 15% of full scale (PFMIN = 1). If PFMIN is not set (to one), the logic clears PFCSS (to zero), marking the pyramid Sun measurement as invalid. It then relies on the flat-mounted CSS cells to give a current measurement of the Sun vector. On the next execution of the controller, the logic will note that the PFCSS flag is cleared and will take the left branch instead of the right.

Note that while "PFMIN" determines whether or not the logic uses the pyramid or flat-mounted CSS cells, the Sun's apparent proximity to the panel normals is a prerequisite for switching to (but not from) the pyramid. For the nominal albedo, the Sun vector returned by the flat-mounted CSS cells is not more than 40° off the true Sun vector. See Fig. 1. (It is Rarely more than 60° off for twice the nominal albedo.) Conversely, the pyramid must be pointed close (well within the 28° field of view) to this albedo to record minimum CSS cell currents from it instead of the Sun. Thus, the agreement of the two sets of cells (flat-mounted and pyramid) prevents the pyramid from becoming stuck on a strong Earth albedo far from the Sun. Moreover, as Clark nears the equator, the flat-mounted CSS cells and algorithm easily discern the Sun from the albedo vector.

Upon exiting eclipse, the Earth albedo is weak and is along the Sun vector. At orbit sunrise, Clark typically will be reeling from the unmitigated disturbances in

eclipse. Clark will need its flat-mounted CSS cells to find a Sun vector that is probably far away from the pyramid's field of view. As Clark works to align its panel normals to the Sun, the Sun will pass within view of the pyramid. Frequently, the CSS logic will switch to the pyramid as the Sun passes over it--but before the controller has reached steady state. Then as Clark's angular momentum carries its panels away from the Sun, the CSS logic will return to the flat-mounted cells to measure the Sun vector. Once the controller has steadied Clark's panel normals relatively near the Sun, the pyramid cells can then measure the Sun vector for the rest of the Sun pass. This solar acquisition typically takes place in approximately 6 minutes. This time is long before the albedo has diverged from the Sun and grown strong enough to cause a 15° error in the flat-mounted cells' measurement of the Sun vector.

Testing this algorithm consisted of checking: the measured Sun vectors, the true Sun vectors, the PFMIN flag, the PFCSS flag, and the conditions that set and clear these flags. The above acquisition scenario appeared in plots and in the on-line debugger of the FORTRAN application package. These same results occurred with both the nominal and worst case (twice nominal) Earth albedo. The simulation was even initialized with the pyramid directly facing the worst case Earth albedo. In this final test, the logic correctly chose the flat-mounted CSS cells to measure the Sun while the controller slewed the spacecraft to acquire the Sun with the pyramid.

Pyramid Configuration Simulation Results

Fig. 7 shows a plot for the combination of pyramid and flat-mounted CSS models and switching logic described above. The simulation for this graph uses the same nominal albedo and orbital conditions as for the simulation of the purely flat-mounted configuration.
The use of both pyramid and flat-mounted CSS cells reduces the average panel-Sun error (averaged over the Sunlit portions of the orbit only) to 8.54°.

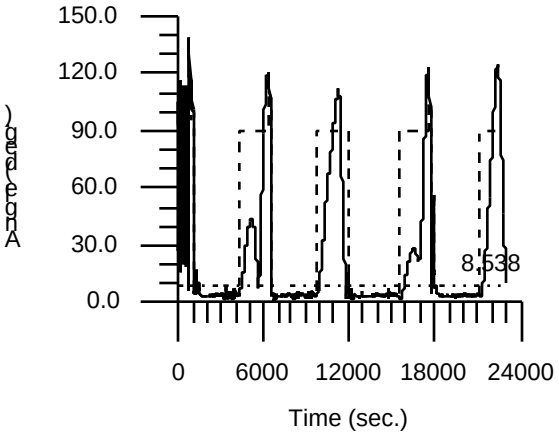

Fig. 7: True & CSS Panel-Sun Angle; Pyramid Configuration.

The final figure, Fig. 8, shows a plot for an increased albedo. This simulation used the same pyramid (and flat-mounted) combination of CSS cells as the previous one. This simulation is identical to the previous one with the exception that the simulation doubles every albedo intensity. It limits resulting albedos greater than 80% to 80%, the maximum albedo in Spacecraft Attitude Determination and Control.[1] These increased albedos cause a 8.55° average Sun error.

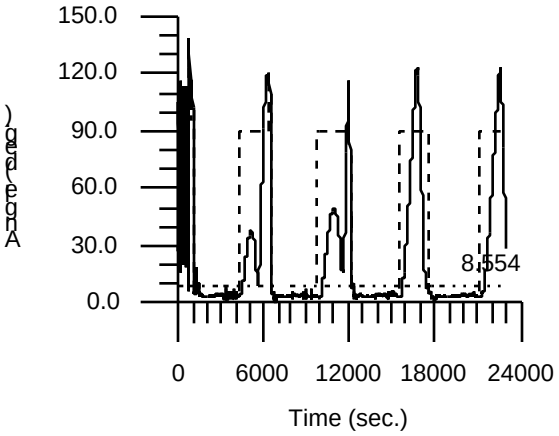

Fig. 8: Panel-Sun Angle; Pyramid Configuration, Doubled Albedo.

Pyramid Thermal Control and Redundancy

Refer to the configuration of the pyramid of CSS cells in Fig. 6. The collar in Fig. 6 is 3 inches high by approximately 5 inches in (inside) diameter. To minimize stray light on the CSS cells, all other areas inside the collar should be flat black. Since a flat black finish will absorb considerable heat from the Sun, the collar diameter should be kept small (while maintaining the same field of view). The 5 inch diameter can be reduced to approximately 3.5 inches without interfering with the corners of the pyramid. One of CTA's thermal engineers estimates that a 3.5 inch diameter assembly would absorb approximately 8 Watts of heat. With a properly insulated mounting, this power would pose no threat to the spacecraft. The cells themselves are designed to run hot.

The scarcity of unobstructed space on the -Z side of the Clark spacecraft further motivates a small pyramid assembly. By placing cells so that a corner of each cell extends up into the top corner of pyramid, the size of the pyramid may be reduced slightly further. This further reduction allows an even smaller diameter collar.
The 3 inch (or less) height of a collar above the base of the pyramid should provide no difficulties. At least 1 inch of this height would be matched by the thickness of the thermal blankets.

Since the Clark spacecraft is limited to 14 CSS channels, the three CSS cells in the pyramid would have to come from the existing cells distributed over the 6 faces of the machine. While the positive and negative Y faces have 3 cells each, all of the remaining faces have only two cells each. The Y faces, however, are subject to shading by the primary and secondary solar arrays. Therefore, while the positive and negative X and Z faces have only one redundant cell each, the Y faces may have less redundancy despite their extra cells. Cells for the pyramid then, would probably best come from the Z, the positive X, and the negative X faces. Then a degraded pointing performance (without the pyramid CSS assembly) would be traded for a loss of redundancy in the flat-mounted CSS cells.

V. Conclusions About Coarse Sun Sensing

Without the pyramid, the safe-hold Sun pointing performance error is 16.3° for the nominal albedo. This error is an average over the Sun-lit portion of the orbits only. It violates the original goal of 10°.

For the pyramid configuration, the average (Sun-lit) panel-Sun error is approximately 8.5°. Thus, the pyramid configuration's pointing performance error is less than the flat-mount configuration's. Moreover, it continually is within the original 10° goal for all albedo approximations.

Error Without Pyramid	~16.3°
Error With Pyramid	~8.5°

Although the pyramid CSS configuration reduces Sun pointing safe-hold performance errors by approximately 50% and is robust to errors from the widely varying albedo, it will not fly on SSTI Clark. At the time that these simulations were run, the need for fairly tight (less than 10°) Sun pointing was thought to be quite profound. Shortly afterwards, though, power consumption measurements were taken of the equipment required for safe-hold mode operation. These measurements reduced the previously estimated consumption by nearly a third.

The trade between pointing performance and CSS redundancy (see section IV's last subsection) depended on the outcome of a power balance study. This study showed that Clark's flat-mounted sensors satisfied the power requirements. With the recent reductions in hardware power requirements, the pointing performance errors were not as damaging as previously thought. Due to the late location

in the project schedule and the corresponding funding, Clark engineers did not implement the pyramid configuration of CSS cells.

Acknowledgments

I would like to thank Walter Grossman at CTA Space Systems for his pyramid advice and for his REX II CSS data analysis.

I would also like to thank Alex Chuchra at CTA Space Systems for his thermal analysis of the pyramid sensor configuration.

References

[1.] Spacecraft Attitude Determination and Control, Wertz, J. R., Ed., Kluwer Academic Publishers, Norwell, Massachusetts, 1978, pp 82 to 83.

[2.] Spencer, Paul R., "Study of a Solar Sensor for Use in Space-Vehicle Orientation Control Systems", NASA Technical Note D-885, National Aeronautics and Space Administration, Washington, 1961.

[3.] Stephens, G. L., Campbell, G. G., and Vonder Haar, T. H., "Earth Radiation Budgets". Journal Of Geophysical Research, Vol. 86, No. C10, October 20, 1981.

[4.] Satellite Thermal Control Handbook, Gilmore, David G., Ed., The Aerospace Corporation Press, El Segundo, California, 1994, pp 2-5 to 2-6.

Jeff Benton earned his Bachelor's and Master's degrees from Columbia University's School of Engineering and Applied Science. He is a member of AIAA. He has worked on Attitude Control Systems at Fairchild Space & Defense, Ithaco Technical Services, and CTA.

Appendix -- Flow Chart of Pyramid and Flat-Mounted CSS Algorithms